

Oxomolybdenum(IV,V,VI) Complexes: Structures, Reactivities, and Criteria of Detection of Binuclear (μ -Oxo)molybdenum(V) Products in Oxygen Atom Transfer Systems

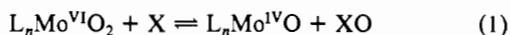
Julia A. Craig,¹ Edgar W. Harlan, Barry S. Snyder, Mark A. Whitener, and R. H. Holm*

Received December 6, 1988

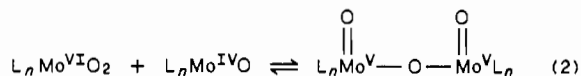
A series of dioxo-Mo(VI) Schiff base complexes of the type $\text{MoO}_2(\text{R-L})(\text{solv})$ has been prepared: L = 2-(salicylideneamino)-phenolate(2-) (sap) or 2-(salicylideneamino)benzenethiolato(2-) (ssp); solv = solvent. Salicylidene ring substituents R were selected to promote solubility and crystallinity. The unsubstituted complexes $\text{MoO}_2(\text{sap})(\text{solv})$ (1) and $\text{MoO}_2(\text{ssp})(\text{solv})$ (3) have been previously reported. The structures of two members of the series were determined. $[\text{MoO}_2(5-t\text{-Busap})(\text{MeOH})]\cdot\text{MeOH}$ (2) crystallizes in space group $P2_1$ with $a = 6.874$ (2) Å, $b = 11.333$ (2) Å, $c = 13.295$ (4) Å, $\beta = 98.79$ (2)°, and $Z = 2$ and was refined to $R = 2.9\%$. $(\text{Me}_4\text{N})[\text{MoO}_2(5\text{-SO}_3\text{ssp})]$ (4) was obtained in space group $P2_1/c$ with $a = 11.156$ (4) Å, $b = 12.747$ (7) Å, $c = 14.055$ (2) Å, $\beta = 97.06$ °, and $Z = 4$ and was refined to $R = 3.8\%$. The two complexes contain the cis MoO_2 group with O-Mo-O angles of 105°. Other structural features include severely distorted octahedral coordination, *mer* disposition of the tridentate ligands, and a weakly bound solv molecule trans to an oxo ligand (2); these attributes apply to Mo(V,IV) complexes as well. Complex 4 is a chain polymer linked by coordination of the sulfonate group trans to an oxo ligand. Reaction of $\text{MoO}_2(\text{R-L})(\text{solv})$ with Ph_2MeP in DMF affords products with UV-visible spectra previously attributed to the Mo(IV) complexes $\text{MoOL}(\text{solv})$. These products have been identified as μ -oxo binuclear Mo(V) complexes by structure determinations. $\text{Mo}_2\text{O}_3\text{-}(3\text{-}t\text{-Buspp})_2(\text{DMF})_2$ (11) crystallizes in space group $Pbca$ with $a = 9.245$ (3) Å, $b = 20.763$ (6) Å, $c = 22.417$ (7) Å, and $Z = 4$, while $[\text{Mo}_2\text{O}_3(3\text{-EtOssp})_2(\text{DMF})_2]\cdot 2\text{DMF}$ (12) was found in space group $P\bar{1}$ with $a = 8.347$ (1) Å, $b = 12.110$ (2) Å, $c = 12.194$ (2) Å, $\alpha = 100.73$ (1)°, $\beta = 93.81$ (1)°, $\gamma = 103.27$ (1)°, and $Z = 1$. The structures were refined to 4.1% (11) and 2.6% (12). Both complexes have imposed centrosymmetry. When the reduction reaction with phosphine was carried out in the presence of 2,2'-bipyridyl, the Mo(IV) products $\text{MoO}(\text{R-L})(\text{bpy})$ (R = H (13), 3-*t*-Bu (14)) were isolated. Compound 14 crystallizes in space group $C2/c$ with $a = 36.348$ (5) Å, $b = 10.256$ (1) Å, $c = 16.102$ (2) Å, $\beta = 97.44$ (1)°, and $Z = 8$; the structure was refined to $R = 8.8\%$. Compound 13 was correctly formulated in an earlier report. Trapping of the $\text{Mo}^{\text{IV}}\text{O}$ state with bpy demonstrates that it is the instantaneous product of reductive atom transfer from the $\text{Mo}^{\text{VI}}\text{O}_2$ oxidation level. In the absence of a trapping reagent, Mo(V) complexes such as 11 and 12 are formed in the rapid, irreversible reaction $\text{MoO}_2(\text{R-L})(\text{solv}) + \text{MoO}(\text{R-L})(\text{solv}) \rightarrow \text{Mo}_2\text{O}_3(\text{R-L})_2(\text{solv})_2$. Criteria for the formation of Mo_2O_3 complexes in solution include demonstration of the reaction stoichiometry $2\text{MoO}_2(\text{R-L})(\text{solv}) + \text{R}_3\text{P} \rightarrow \text{Mo}_2\text{O}_3(\text{R-L})_2(\text{solv})_2 + \text{R}_3\text{PO}$ by ^{31}P NMR, detection of diastereomers, and characteristic absorption spectra. An additional criterion follows from proof of the reaction stoichiometry $\text{Mo}_2\text{O}_3(\text{R-L})_3(\text{solv})_2 + (\text{R}_F)_2\text{SO} \rightarrow 2\text{MoO}_2(\text{R-L})(\text{solv}) + (\text{R}_F)_2\text{S}$ by ^{19}F NMR ($\text{R}_F = p\text{-C}_6\text{H}_4\text{F}$). Because in a variety of solvents no Mo(V) complex undergoes detectable dissociation, it is probable that the foregoing reaction involves the intact Mo_2O_3 and proceeds by coordination of sulfoxide to the Mo followed by intramolecular atom and electron transfer. The results of this work emphasize the pervasiveness of formation of Mo_2O_3 species in oxo transfer reaction systems.

Introduction

Molybdenum-mediated oxygen atom transfer reactions have become increasingly well-defined with regard to scope, kinetics, and mechanisms since the first report of their occurrence in 1972, in the form of atom transfer from Mo(VI) to tertiary phosphines.² A recent account of these reactions is available.³ Contemporary research on oxo transfer in these laboratories⁴⁻¹¹ and elsewhere¹²⁻¹⁵ has been stimulated by the prospect of catalytic oxidation of substrates and by the problem of interpreting the mechanism of action of the molybdenum hydroxylases or, alternatively, oxo-transferases.⁹ The forward and reverse reactions 1 have been



amply demonstrated with a number of substrates X/XO, and a thermodynamic reactivity scale has been devised.^{3,7} Oxo transfer is accompanied by the formation of a μ -oxo dimer in reaction 2, which, from current evidence, occurs unless it is sterically prevented.

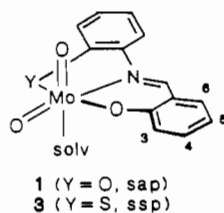


While reaction 2 has been prevented in systems containing sterically encumbered Mo(VI,IV) complexes,^{6-11,15} it is otherwise pervasive, and both reversible and irreversible examples are known. This reaction has been the most thoroughly characterized with dithiocarbamate complexes ($\text{L} = \text{R}_2\text{NCS}_2^-$, $n = 2$), for which it is reversible.^{3,16} From this and other reactions, over 20 complexes containing the diamagnetic $[\text{Mo}_2\text{O}_3]^{4+}$ core in the syn or anti conformation have been isolated and structurally identified.¹⁷⁻²¹

- (1) National Science Foundation Predoctoral Fellow, 1986-1987.
- (2) Barral, R.; Bocard, C.; Serée de Roch, I.; Sajas, L. *Tetrahedron Lett.* **1972**, 1693.
- (3) Holm, R. H. *Chem. Rev.* **1987**, *87*, 1401.
- (4) Holm, R. H.; Berg, J. M. *Pure Appl. Chem.* **1984**, *56*, 1645.
- (5) Reynolds, M. S.; Berg, J. M.; Holm, R. H. *Inorg. Chem.* **1984**, *23*, 3057.
- (6) Berg, J. M.; Holm, R. H. *J. Am. Chem. Soc.* **1985**, *107*, 925.
- (7) Harlan, E. W.; Berg, J. M.; Holm, R. H. *J. Am. Chem. Soc.* **1986**, *108*, 6992.
- (8) Caradonna, J. P.; Harlan, E. W.; Holm, R. H. *J. Am. Chem. Soc.* **1986**, *108*, 7856.
- (9) Holm, R. H.; Berg, J. M. *Acc. Chem. Res.* **1986**, *19*, 363.
- (10) Caradonna, J. P.; Reddy, P. R.; Holm, R. H. *J. Am. Chem. Soc.* **1988**, *110*, 2139.
- (11) Craig, J. A.; Holm, R. H. *J. Am. Chem. Soc.* **1989**, *111*, 2111.
- (12) (a) Topich, J.; Lyon, J. T., III. *Inorg. Chim. Acta* **1983**, *80*, L41. (b) Topich, J.; Lyon, J. T., III. *Polyhedron* **1984**, *3*, 55, 61.
- (13) Topich, J.; Lyon, J. T., III. *Inorg. Chem.* **1984**, *23*, 3202.
- (14) Deli, J.; Speier, G. *Transition Met. Chem.* **1981**, *6*, 227.
- (15) Roberts, S. A.; Young, C. G.; Cleland, W. E., Jr.; Ortega, R. B.; Enemark, J. H. *Inorg. Chem.* **1988**, *27*, 3044.

- (16) Matsuda, T.; Tanaka, K.; Tanaka, T. *Inorg. Chem.* **1979**, *18*, 454.
- (17) Garner, C. D.; Howlader, N. C.; Mabbs, F. E.; McPhail, A. T.; Onan, K. D. *J. Chem. Soc., Dalton Trans.* **1979**, 962.
- (18) Lincoln, S.; Koch, S. A. *Inorg. Chem.* **1986**, *25*, 1594.
- (19) (a) Blake, A. B.; Cotton, F. A.; Wood, J. S. *J. Am. Chem. Soc.* **1964**, *86*, 3024. (b) Ricard, L.; Estienne, J.; Karagiannidis, P.; Toledano, P.; Fischer, J.; Mitschler, A.; Weiss, R. *J. Coord. Chem.* **1974**, *3*, 227. (c) Zubieta, J. A.; Maniloff, G. B. *Inorg. Nucl. Chem. Lett.* **1976**, *12*, 121. (d) Tatsumisago, M.; Matsubayashi, G.; Tanaka, T.; Nishigaki, S.; Nakatsu, K. *J. Chem. Soc., Dalton Trans.* **1982**, 121.
- (20) (a) Dahlstrom, P. L.; Hyde, J. R.; Vella, P. A.; Zubieta, J. *Inorg. Chem.* **1982**, *21*, 927. (b) Cotton, F. A.; Fanwick, P. E.; Fitch, J. W., III. *Inorg. Chem.* **1978**, *17*, 3254. (c) Baird, D. M.; Rheingold, A. L.; Croll, S. D.; DiCenso, A. T. *Inorg. Chem.* **1986**, *25*, 3458. (d) Knox, J. R.; Prout, C. K. *Acta Crystallogr.* **1969**, *B25*, 2281. (e) Mattes, R.; Scholand, H.; Mikloweit, U.; Schrenk, V. *Z. Naturforsch.* **1987**, *42B*, 599.

Among the complexes utilized in the recent development of oxo transfer, the Schiff base complexes MoO₂(sap)(solv)²² (**1**) and



MoO₂(ssp)(solv) (**3**), in the work of Topich and Lyon,^{12,13} have played a significant role. Rate constants and activation parameters for oxidation of tertiary phosphines have been determined, it has been shown that rates correlate with Mo(VI) irreversible reduction potentials, and a donor atom reactivity series has been formulated. Products of the reactions with phosphines have been represented as Mo^{IV}O complexes, primarily because of the occurrence of a tight isosbestic point near 400 nm, as in the reduction of **3** with Ph₂EtP in DMF.^{12,13} The possibility of Mo₂O₃ complex formation was recognized. Reaction products were not isolated, but prior to this work Boyd and Spence²³ reported the preparation of a number of Schiff base complexes formulated as Mo^{IV}O compounds. In our examination of the reaction product of **3** with phosphine and of the reaction of a putative Mo^{IV}O-ssp complex with nitrate, we made several observations that encouraged a more detailed examination than heretofore of the reduction products of complexes of types **1** and **3** by atom transfer. We report here the results of that investigation, which include structural characterizations of Mo reactants and products, detection of isomeric Mo(V) complexes, and examples of new oxo transfer reactions. This work provides useful criteria for the detection of Mo^VO₃ complexes formed in reaction 2.

Experimental Section

Preparation of Compounds. 3-Ethoxysalicylaldehyde, *o*-aminothiophenol, methyldiphenylphosphine, ethyldiphenylphosphine, and triethylphosphine were commercial samples and were used as received. The Duff reaction²⁴ was used to prepare 3-*tert*-butylsalicylaldehyde, which was readily separated from a dialdehyde product by flash chromatography with 8% ethyl acetate/92% hexane eluant. 5-*tert*-Butylsalicylaldehyde was also prepared by the Duff reaction. MoO₂(sap),²³ MoO₂(ssp),²³ Mo₂O₃(acac)₄,²⁵ and bis(*p*-fluorophenyl) sulfide and sulfide²⁶ were obtained by published methods.

(a) **Ligands.** H₂(5-*t*-Busap).²² An ice-cooled solution of 2.70 g (16 mmol) of 5-*tert*-butylsalicylaldehyde in ethanol was treated with 1.75 g (16 mmol) of *o*-aminophenol. The reaction mixture was stirred for 1 h and cooled to -20 °C. The orange crystalline solid was collected, washed with cold ethanol, and dried in vacuo to afford 3.6 g (84%) of product. ¹H NMR (CDCl₃): δ 1.33 (s, 9), 6.9–7.5 (m, 7), 8.70 (s, 1, HCN).

The ligands described below are named as Schiff bases²² for simplicity, even though they were obtained in the thiazoline form as determined by their ¹H NMR spectra.²⁷ This form lacks the characteristic azomethine resonance at δ 8.5–9.5²⁸ and instead displays a methine signal at δ 5.5–6.5.

- (21) (a) Bino, A.; Cohen, S.; Tsimering, L. *Inorg. Chim. Acta* **1983**, *77*, L79. (b) Hyde, J. R.; Zubieta, J. *Cryst. Struct. Commun.* **1982**, *11*, 929. (c) Tsao, Y. Y.-P.; Fritchie, C. J., Jr.; Levy, H. A. *J. Am. Chem. Soc.* **1978**, *100*, 4089. (d) Kamenar, B.; Penavic, M.; Korpar-Colig, B.; Markovic, B. *Inorg. Chim. Acta* **1982**, *65*, L245. (e) El-Essawi, M. M.; Weller, F.; Stahl, K.; Kersting, M.; Dehnicke, K. *Z. Anorg. Allg. Chem.* **1986**, *542*, 175.
- (22) Abbreviations: acac = acetylacetonate(1-); bpy = 2,2'-bipyridyl; cat = catecholate(2-); hfac = hexafluoroacetylacetonate(1-); phen = 1,10-phenanthroline; sap = 2-(salicylideneamino)phenolate(2-); solv = solvent; ssp, 2-(salicylideneamino)benzenethiolate(2-).
- (23) Boyd, I. W.; Spence, J. T. *Inorg. Chem.* **1982**, *21*, 1602.
- (24) Duff, J. C. *J. Chem. Soc.* **1941**, 547.
- (25) Chen, G. J.-J.; McDonald, J. W.; Newton, W. E. *Inorg. Chem.* **1976**, *15*, 2612.
- (26) (a) Leonard, N. J.; Sutton, L. E. *J. Am. Chem. Soc.* **1948**, *70*, 1564. (b) Wilson, G. E., Jr.; Chang, M. M. *J. Am. Chem. Soc.* **1974**, *96*, 7533.
- (27) Alyea, E. C.; Malek, A. *Can. J. Chem.* **1974**, *53*, 939.
- (28) O'Connor, M. J.; Ernst, R. E.; Schoenborn, J. E.; Holm, R. H. *J. Am. Chem. Soc.* **1968**, *90*, 1744.

Na(5-SO₃ssp). Sodium salicylaldehyde-5-sulfonate²⁹ (20.0 g, 89 mmol), and *o*-aminobenzenethiol (11 mL, 100 mmol) were combined in 80 mL of ethanol/water (1:1 v/v) and vigorously stirred for 20 min, during which time the reactants dissolved and a pale yellow solid subsequently precipitated. The product was collected, washed with ether, and dried in air to afford 14.5 g (49%). A small second crop could be obtained by storing the filtrate at -20 °C. ¹H NMR (D₂O): δ 6.43 (s, 1), 6.80–7.13 (m, 5), 7.60 (d, 2), 7.80 (s, 1).

(R₄N)(5-SO₃ssp). The Me₄N⁺ and *n*-Pr₄N⁺ salts were obtained by combining 3.0 g (9.1 mmol) of Na(5-SO₃ssp) and 11 mmol of R₄NCl in 20 mL of water. The reaction mixture was stirred for 30 min, and the white precipitate was filtered, washed with ice water, ethanol, and ether, and dried in vacuo to afford the product (80–90%). This material was suitable for use in the reactions below. The compounds may be obtained as white needles by recrystallization from hot methanol (Me₄N⁺ salt), and as white microcrystals from methanol/water (*n*-Pr₄N⁺ salt). ¹H NMR (Me₂SO-*d*₆): δ 6.50–6.82 (m, 6), 7.33 (d, 1), 7.72 (s, 1), 9.97 (s, 1). This and the following compound discolor at room temperature and should be stored in a freezer.

H₂(3-*t*-Bussp). A mixture of 3.15 g (17.7 mmol) of 3-*tert*-butylsalicylaldehyde and 1.89 mL (17.7 mmol) of *o*-aminobenzenethiol in 8 mL of methanol was stirred for 20 min. Storage of the yellow solution overnight at room temperature and then at -20 °C for 24 h caused separation of white crystals, which were collected and washed with hexane to afford 3.77 g (75%) of product. ¹H NMR (CDCl₃): δ 1.43 (s, 9), 4.62 (br s, 1), 6.75–7.05 (m, 5), 7.13 (d, 2), 7.31 (d, 2), 9.45 (s, 1).

Complexes. [MoO₂(5-*t*-Busap)(MeOH)]·MeOH (**2**). To a stirred solution of 4.00 g (12 mmol) of MoO₂(acac)₂³⁰ in 60 mL of methanol was added 3.30 g (12 mmol) of H₂(5-*t*-Busap). The solution quickly turned orange and a solid separated. It was stirred for 1 h, and maintained at -20 °C overnight. The solid was collected, washed with cold methanol, and dried in vacuo to afford 4.30 g (76%) of product as an orange crystalline solid. ¹H NMR (Me₂SO-*d*₆): δ 1.33 (s, 9), 3.15 (s, 6, MeOH), 4.08 (br s, 2, MeOH), 6.80–7.75 (m, 7), 9.32 (s, 1, HCN). Prior to analysis the compound was heated at 40 °C for 16 h to remove methanol. Anal. Calcd for C₁₇H₁₇MoNO₄: C, 51.67; H, 3.58; Mo, 24.27; N, 4.22. Found: C, 51.66; H, 3.54; Mo, 24.26; N, 4.34.

(Me₄N)[MoO₂(5-SO₃ssp)] (**4a**). (Me₄N)(5-SO₃ssp) (4.13 g, 10.8 mmol) and MoO₂(acac)₂ (3.52 g, 10.8 mmol) were dissolved in 60 mL of methanol and stirred for 6 h, during which a dark orange precipitate separated. This material was collected, washed with methanol and ether, and dried in vacuo to afford 4.90 g (89%) of product, which was used in a crystal structure determination.

(*n*-Pr₄N)[MoO₂(5-SO₃ssp)] (**4b**). (*n*-Pr₄N)(5-SO₃ssp) (8.05 g, 16.0 mmol) and MoO₂(acac)₂ (5.31 g, 16.0 mmol) were dissolved in 50 mL of methanol/ethanol (1:1 v/v) and the mixture was stirred for 1 h. The reaction mixture was cooled at -20 °C for several hours and filtered. The orange solid was washed with ether to give 7.2 g (72%) of product. This material was recrystallized from methanol/ethanol (4:1 v/v) with addition of ether to the turbidity point, affording the product as orange microcrystals. ¹H NMR (Me₂SO-*d*₆): δ 0.87 (t, 12), 1.59 (m, 8), 3.12 (q, 8), 6.82 (d, 1), 7.10–7.29 (m, 3), 7.68–7.77 (m, 2), 8.11 (s, 1), 9.13 (s, 1, HCN). IR (DMF): ν_{MoO} 901, 932 cm⁻¹. Anal. Calcd for C₂₂H₃₆MoN₂O₆S₂: C, 48.38; H, 5.85; Mo, 15.46; N, 4.51; S, 10.33. Found: C, 48.63; H, 6.08; Mo, 15.51; N, 4.53; S, 10.44.

MoO₂(3-OEtssp) (**5**). The ligand H₂(3-OEtssp) was prepared by the reaction of 3-ethoxysalicylaldehyde and *o*-aminobenzenethiol in ethanol and was identified by its ¹H NMR spectrum. A solution of 5.0 g (18 mmol) of H₂(3-OEtssp) and 5.9 g (20 mmol) of MoO₂(acac)₂ was stirred in 100 mL of methanol for 1 h. The product was collected by filtration, washed with methanol, and dried in vacuo. This material was recrystallized from Me₂SO/H₂O and dried in vacuo to afford 6.15 g (86%) of product as an unsolvated brown microcrystalline solid. ¹H NMR (Me₂SO-*d*₆): δ 1.32 (t, 3), 4.04 (q, 2), 6.94 (t, 1), 7.11–7.30 (m, 4), 7.40 (d, 1), 7.69 (d, 1), 9.04 (s, HCN, 1). Anal. Calcd for C₁₅H₁₃MoNO₄S: C, 45.12; H, 3.28; Mo, 23.83; N, 3.51; S, 8.03. Found: C, 45.00; H, 3.26; Mo, 23.76; N, 3.47; S, 8.40.

MoO₂(3-*t*-Bussp) (**6**). A mixture of 1.00 g (3.50 mmol) of H₂(3-*t*-Bussp) and 1.14 g (3.50 mmol) of MoO₂(acac)₂ in 25 mL of *tert*-butyl alcohol was stirred and heated to 65 °C. After 5 min at this temperature, it was cooled to room temperature. The mixture was allowed to stand for an additional 30 min, after which a microcrystalline brown solid was collected by filtration and was washed with *tert*-butyl alcohol (5 mL) and

- (29) (a) Botsivali, M.; Evans, D. F.; Missen, P. H.; Upton, M. W. *J. Chem. Soc., Dalton Trans.* **1985**, 1147. (b) Berry, K. J.; Moya, F.; Murray, K. S.; van den Bergen, A. M.; West, B. O. *J. Chem. Soc., Dalton Trans.* **1982**, 109.
- (30) Jones, M. M. *J. Am. Chem. Soc.* **1959**, *81*, 3188.

Table I. Crystallographic Data for Mo^{VI}O₂ (**2**, **4a**), Mo^VO₃ (**11**, **12**), and Mo^{IV}O (**14**) Complexes

	2	4a	11	12	14
formula	C ₁₉ H ₂₅ MoNO ₆	C ₁₇ H ₂₀ MoN ₂ O ₆ S ₂	C ₄₀ H ₄₈ Mo ₂ N ₄ O ₇ S ₂	C ₄₂ H ₅₄ Mo ₂ N ₆ O ₁₁ S ₂	C ₂₅ D ₃ H ₂₅ MoN ₄ O ₂ S
fw	459.34	508.42	952.86	1074.96	595.96
a, Å	6.874 (2)	11.156 (4)	9.245 (3)	8.347 (1)	36.348 (5)
b, Å	11.333 (2)	12.747 (7)	20.763 (6)	12.110 (2)	10.256 (1)
c, Å	13.295 (4)	14.055 (2)	22.417 (7)	12.194 (2)	16.102 (2)
α, deg				100.73 (1)	
β, deg	98.79 (2)	97.06 (2)		93.81 (1)	97.44 (1)
γ, deg				103.27 (1)	
V, Å ³	1023.5 (4)	1983 (1)	4303 (2)	1171.0 (4)	5952 (1)
Z	2	4	4	1	8
space group	P2 ₁	P2 ₁ /c	Pbca	P $\bar{1}$	C2/c
ρ _{calcd} , g cm ⁻³ (ρ _{obsd} , g cm ⁻³)	1.49 (1.48)	1.70 (1.69)	1.47 (1.46)	1.52 (1.52)	1.32 ^b
μ, cm ⁻¹	7.7	8.8	7.1	6.7	5.3
R(F _o), %	2.87	3.80	4.13	2.58	8.80
R _w (F _o ²), %	3.68	4.77	3.83	4.07	7.56

^a T = 298 K, λ = 0.71069 Å (Mo Kα). ^b Accurate density could not be determined.

hexanes (3 × 10 mL). This material was dried in vacuo to afford 1.10 g (76%) of the product as a brown solid. ¹H NMR (THF-*d*₈): δ 1.41 (s, 9), 6.97 (t, 1), 7.10 (m, 1), 7.16 (t, 1), 7.33 (d, 1), 7.90 (m, 3), 9.15 (s, 1, HCN). The brown material can be recrystallized from Me₂SO/water to yield the microcrystalline orange Me₂SO adduct, which was analyzed. Anal. Calcd for C₁₉H₂₃MoNO₄S₂: C, 46.62; H, 4.74; Mo, 19.60; N, 2.86; S, 13.10. Found: C, 46.52; H, 4.52; Mo, 19.18; N, 2.79; S, 13.51.

In the following preparations of Mo(V,IV) complexes, all operations were conducted under a pure dinitrogen atmosphere and solvents were dried and degassed prior to use. The nature of complexes **7** and **9** is discussed in the text. The complex Mo₂O₃(5-*t*-Busap)₂ (**8**) was generated in solution by reduction of **2** with Ph₂MeP but was not isolated.

(*n*-Pr₄N)₂[Mo₂O₃(5-SO₃ssp)₂(DMF)₂] (**10**). (*n*-Pr₄N)[MoO₂(5-SO₃ssp)] (**4b**; 5.0 g, 8.1 mmol) was dissolved in a minimum volume (ca. 80 mL) of DMF at 70 °C. After the solution was cooled to room temperature, 3.45 mL (16 mmol) of Ph₂EtP in 80 mL of ethanol was introduced. The solution was stirred overnight, an equal volume of ether was added, and the mixture was maintained at -20 °C overnight. The solid was collected, washed with ether/ethanol (1:1 v/v), and dried in vacuo to afford the product (4.25 g, 69%) as highly dioxygen-sensitive, dark brown microcrystals. ¹H NMR (anion, CD₃OD): δ 0.90 (t, 12), 7.20 (m, 3), 7.48 (m, 1), 7.84 (d, 1), 7.97 (m + DMF), 8.17 (t, 1), 9.29 + 9.32 (s, s, 1, HCN). IR (DMF): ν_{MoO} 957 cm⁻¹. Anal. Calcd for C₂₆H₈₆Mo₂N₆O₁₃S₄: C, 49.04; H, 6.32; Mo, 13.99; N, 6.13; S, 9.37. Found: C, 49.39; H, 6.53; Mo, 14.36; N, 6.25; S, 9.34.

Mo₂O₃(3-*t*-Bussp)₂(DMF)₂ (**11**). MoO₂(3-*t*-Bussp) (**6**; 0.78 g, 1.89 mmol) was dissolved in 25 mL of DMF, and 380 μL (1.90 mmol) of Ph₂MeP was added. The solution was stirred at 70 °C for 30 min, during which time the color darkened to deep red. While the solution was still warm, 25 mL of methanol was added. The solution was stored at -20 °C overnight, and the solid which separated was collected, washed with methanol and ether, and dried in vacuo. The product was obtained as 0.61 g (68%) of a red-brown microcrystalline solid. ¹H NMR (THF-*d*₈): 1.64 (s, 9), 6.85 (t, 1), 7.11 (m, 1), 7.18 (m, 1), 7.46 (d, 1), 7.57 (d, 1), 7.62 (d, 1), 7.73 (d, 1), 9.27 (s, 1, HCN). IR (DMF): ν_{MoO} 954 cm⁻¹. Anal. Calcd for C₄₀H₄₈Mo₂N₄O₇S₂: C, 50.42; H, 5.08; Mo, 20.14; N, 5.88; S, 6.73. Found: C, 50.49; H, 5.18; Mo, 19.81; N, 5.92; S, 7.09.

Mo₂O₃(3-EtOssp)₂(DMF)₂ (**12**). MoO₂(3-EtOssp) (**5**; 3.0 g, 7.5 mmol) was dissolved in the minimum amount of DMF at 50 °C. To this solution was added 3.0 mL (14.8 mmol) of Ph₂MeP in 40 mL of acetonitrile. The reaction mixture was stirred for 5 h and stored at -20 °C overnight. The solid was collected by filtration, washed with acetonitrile and ether, and dried in vacuo to afford 3.2 g (99%) of product as a fine red-brown powder. IR (KBr): ν_{MoO} 945 cm⁻¹. Anal. Calcd for C₃₆H₄₀Mo₂N₄O₈S₂: C, 46.55; H, 4.34; Mo, 20.67; N, 6.03; S, 6.90. Found: C, 47.05; H, 4.38; Mo, 20.76; N, 6.10; S, 7.33.

MoO(3-*t*-Bussp)(bpy) (**14**). To a mixture of 0.256 g (0.620 mmol) of MoO₂(3-*t*-Bussp) (**6**) and 0.900 g (5.77 mmol) of 2,2'-bipyridyl in 25 mL of THF was added 180 μL (0.950 mmol) of Ph₂MeP. The mixture was refluxed for 2 h, during which time the color darkened and became green. The solution volume was reduced to ca. 6 mL (without separation of solid), 20 mL of methanol was added and the solution was stored at -20 °C for 2 days. The material that separated was collected, washed with ether, and dried in vacuo to afford 0.15 g (44%) of a green-black crystalline solid. ¹H NMR (THF-*d*₈): δ 0.87 (s, 9), 6.54 (t, 1), 6.92 (t, 1), 7.00 (t, 1), 7.07 (t, 1), 7.13 (t, 1), 7.21 (d, 1), 7.41 (d, 1), 7.48 (d, 1), 7.56 (t, 1), 7.68 (t, 1), 7.80 (d, 1), 7.96 (d, 1), 8.29 (d, 1), 8.38 (d, 1), 9.17 (d, 1), 9.30 (s, 1, HCN). Anal. Calcd for C₂₇H₂₅MoN₃O₂S:

C, 58.80; H, 4.57; Mo, 17.40; N, 7.62; S, 5.81. Found: C, 57.84; H, 4.17; Mo, 17.07; N, 7.74; S, 5.94.

Collection and Reduction of X-ray Data. Diffraction-quality crystals were obtained as follows: **2** (orange), by slow cooling of a saturated methanol solution; **4a** (ruby red), by ether diffusion into a concentrated methanol solution; **11** (dark red), from the anaerobic reaction of MoO₂(3-*t*-Bussp) (25 mM) and Ph₂EtP (35 mM) in THF followed by the addition of acetonitrile (25% v/v) and by allowing the solution to stand for several days; **12** (dark red), from an anaerobic saturated DMF solution initially at 70 °C that was allowed to stand for several weeks at room temperature; **14** (black), from the reaction mixture to which had been added CD₃CN (15% v/v) by allowing the solution to stand for several days in an NMR tube. Crystals of **2** and **4a** were mounted in glass capillaries; crystals of the remaining compounds were sealed under dinitrogen. Data were collected on a Nicolet P3F diffractometer. For all compounds except **14**, space groups were uniquely determined by axial symmetries determined from rotation photographs and systematic absences. The centrosymmetric space group C2/c for **14** was favored by simple *E* statistics, a choice confirmed by successful solution and refinement of the structure. For each crystal, unit cell parameters were determined from 25 machine-centered reflections over 20° ≤ 2θ ≤ 25°. Three check reflections registered every 123 reflections indicated no significant decay during data collections. The data were processed by using XTape of the SHELXTL program package (Nicolet XRD Corp., Madison, WI), and empirical absorption corrections were applied with the program PSICOR. Crystallographic data for the five compounds are contained in Table I.

Structure Solutions and Refinements. Atom scattering factors were taken from a standard source.³¹ Patterson methods were used to locate the Mo atom in **4a**. For the other compounds, Mo atoms and partial coordination spheres were determined by direct methods (MULTAN). All other non-hydrogen atoms were located in successive Fourier maps and difference Fourier maps and were refined with the program CRYSTALS. For **11** and **12**, the bridging oxygen atoms were fixed with half-occupancy on inversion centers. The cation in **4a** exhibited large thermal parameters indicative of disorder and was refined isotropically. Isotropic refinements converged at *R* values of 8.2% (**2**), 11.3% (**4a**), 8.6% (**11**), 8.2% (**12**), and 12.9% (**14**). Because of data limitations, phenyl carbon atoms and the solvate molecule of **11** were refined isotropically. All other non-hydrogen atoms in the five compounds were described anisotropically. In the final stages of refinement, hydrogen atoms were placed at 0.95 Å from and assigned isotropic thermal parameters 1.2× those of adjacent carbon atoms. Final *R* factors are given in Table I; positional parameters are collected in Tables II–VI.³²

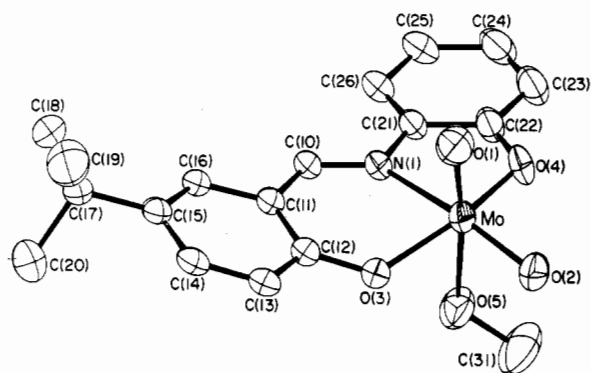
Other Physical Measurements. All measurements were made under anaerobic conditions. Absorption spectra were obtained on a Cary 219 or a Perkin Elmer Lambda 4C spectrophotometer. ¹H NMR spectra were recorded on Bruker AM spectrometers operating at 250–500 MHz; ³¹P spectra were acquired at 121.54 MHz, and shifts are referenced to an external 85% H₃PO₄/D₂O (pH 7) reference; solutions contained ca. 10% (v/v) CD₃CN for the deuterium lock. Appropriate repetition times were used to allow accurate signal integrations. ¹⁹F NMR measurements were made as previously described;¹⁰ chemical shifts were referenced to

(31) Cromer, D. T.; Waber, J. T. *International Tables for X-Ray Crystallography*; Kynoch Press: Birmingham, England, 1974.

(32) See paragraph at end of paper concerning supplementary material available.

Table II. Atom Positional Parameters ($\times 10^4$) for $\text{MoO}_2(5-t\text{-Busap})(\text{MeOH})\cdot\text{MeOH}$

atom	x/a	y/b	z/c
Mo(1)	2186	5094	2973
N(1)	-776 (3)	4768 (2)	3478 (1)
O(1)	3078 (3)	3746 (2)	3353 (2)
O(2)	4152 (3)	5827 (2)	2619 (2)
O(3)	697 (3)	4627 (2)	1682 (1)
O(4)	2358 (3)	5863 (2)	4305 (2)
O(5)	500 (4)	6859 (2)	2482 (2)
O(6)	7047 (4)	7522 (3)	2962 (2)
C(2)	6959 (9)	8160 (5)	3861 (5)
C(10)	-2170 (3)	4106 (2)	3019 (2)
C(11)	-2094 (3)	3526 (2)	2066 (1)
C(12)	-654 (3)	3778 (2)	1452 (2)
C(13)	-677 (4)	3137 (3)	555 (2)
C(14)	-2042 (4)	2256 (3)	292 (2)
C(15)	-3502 (4)	1980 (2)	891 (2)
C(16)	-3514 (3)	2647 (2)	1762 (1)
C(17)	-4989 (4)	1012 (2)	562 (2)
C(18)	-6385 (7)	792 (4)	1336 (3)
C(19)	-6300 (6)	1392 (4)	-444 (3)
C(20)	-3953 (8)	-128 (3)	358 (4)
C(21)	-875 (3)	5260 (2)	4447 (1)
C(22)	886 (4)	5815 (2)	4863 (2)
C(23)	1060 (5)	6317 (3)	5825 (2)
C(24)	-511 (6)	6262 (3)	6363 (2)
C(25)	-2284 (5)	5734 (3)	5940 (2)
C(26)	-2465 (4)	5226 (3)	4979 (2)
C(31)	1424 (8)	7975 (4)	2551 (5)

**Figure 1.** Structure of $[\text{MoO}_2(5-t\text{-Busap})(\text{MeOH})]\cdot\text{MeOH}$ (**2**) as its methanol solvate, showing 50% probability ellipsoids and the atom-labeling scheme.

CFCl_3 external standard. Infrared spectra were obtained with a Nicolet 5ZDX spectrophotometer. FAB mass spectra were taken in 3-nitrobenzyl alcohol by using a Kratos MS50 spectrometer equipped with a xenon gun.

Results and Discussion

The Schiff base complexes **1–14** are of primary interest in this investigation, and include the oxidation states Mo(VI) (**1–6**),

$\text{MoO}_2(\text{sap})(\text{solv})$	1
$\text{MoO}_2(5-t\text{-Busap})(\text{solv})$	2
$\text{MoO}_2(\text{ssp})(\text{solv})$	3
$(\text{Me}_4\text{N})[\text{MoO}_2(5\text{-SO}_3\text{ssp})]$	4a
$(n\text{-Pr}_4\text{N})[\text{MoO}_2(5\text{-SO}_3\text{ssp})(\text{solv})]$	4b
$\text{MoO}_2(3\text{-EtOssp})(\text{solv})$	5
$\text{MoO}_2(3-t\text{-Bussp})(\text{solv})$	6
$\text{Mo}_2\text{O}_3(\text{sap})_2(\text{solv})_2$	7
$\text{Mo}_2\text{O}_3(5-t\text{-Busap})_2(\text{solv})_2$	8
$\text{Mo}_2\text{O}_3(\text{ssp})_2(\text{solv})_2$	9
$(n\text{-Pr}_4\text{N})_2[\text{Mo}_2\text{O}_3(5\text{-SO}_3\text{ssp})(\text{solv})_2]$	10
$\text{Mo}_2\text{O}_3(3-t\text{-Bussp})_2(\text{solv})_2$	11
$\text{Mo}_2\text{O}_3(3\text{-OEtssp})_2(\text{solv})_2$	12
$\text{MoO}(\text{ssp})(\text{bpy})$	13
$\text{MoO}(3-t\text{-Bussp})(\text{bpy})$	14

Mo(V) (**7–12**), and Mo(IV) (**13**, **14**). Complexes **1** and **2**,³³

Table III. Atom Positional Parameters ($\times 10^4$) for $\text{Me}_4\text{N}[\text{MoO}_2(5\text{-SO}_3\text{ssp})]$

atom	x/a	y/b	z/c
Mo(1)	2514.2 (3)	-559.2 (3)	-1417.7 (2)
O(1)	3928 (3)	-629 (3)	-819 (2)
O(2)	2302 (4)	727 (2)	-1711 (2)
S(1)	3082 (1)	-916.4 (9)	-2983.8 (7)
O(3)	1610 (3)	-731 (2)	-324 (2)
N(1)	2420 (3)	-2361 (2)	-1467 (2)
C(10)	1822 (3)	-2920 (3)	-931 (3)
C(11)	1251 (3)	-2567 (3)	-121 (3)
C(12)	1188 (3)	-1507 (3)	165 (3)
C(13)	661 (4)	-1258 (3)	987 (3)
C(14)	229 (4)	-2042 (3)	1531 (3)
C(15)	295 (3)	-3092 (3)	1256 (3)
C(16)	792 (4)	-3347 (3)	441 (3)
C(21)	3038 (3)	-2881 (3)	-2170 (3)
C(22)	3384 (3)	-2264 (3)	-2916 (3)
C(23)	3972 (4)	-2741 (4)	-3619 (3)
C(24)	4258 (4)	-3789 (4)	-3570 (4)
C(25)	3963 (5)	-4376 (4)	-2815 (4)
C(26)	3352 (4)	-3939 (4)	-2113 (4)
S(10)	-231 (1)	-4099.4 (8)	1967.7 (7)
O(11)	-1442 (3)	-3815 (3)	2103 (3)
O(12)	555 (3)	-4062 (2)	2890 (2)
O(13)	-114 (4)	-5073 (3)	1466 (2)
N(30)	7134 (4)	-2534 (3)	-880 (3)
C(30)	7746 (9)	-1516 (8)	-661 (7)
C(31)	8099 (9)	-3270 (8)	-1061 (7)
C(32)	6364 (8)	-2469 (7)	-1826 (6)
C(33)	6567 (14)	-2918 (12)	-115 (11)

Table IV. Atom Positional Parameters ($\times 10^4$) for $\text{Mo}_2\text{O}_3(3-t\text{-Bussp})_2(\text{DMF})_2$

atom	x/a	y/b	z/c
O(2)	5000	0	5000
Mo(1)	5805.1 (5)	60.8 (2)	5770.4 (2)
O(1)	7457 (5)	364 (2)	5626 (2)
S(1)	6295 (2)	-1070.0 (8)	5777.8 (9)
N(1)	6206 (4)	-69 (2)	6714 (2)
O(3)	4743 (5)	881 (2)	6002 (2)
C(10)	5708 (8)	302 (3)	7120 (3)
C(11)	4844 (8)	871 (3)	7064 (3)
C(12)	4424 (7)	1150 (3)	6520 (3)
C(13)	3584 (8)	1730 (3)	6518 (3)
C(14)	3252 (9)	1996 (4)	7063 (4)
C(15)	3669 (11)	1735 (4)	7605 (4)
C(16)	4449 (10)	1180 (4)	7608 (3)
C(21)	7070 (6)	-618 (3)	6888 (3)
C(22)	7136 (6)	-1124 (3)	6481 (3)
C(23)	7949 (8)	-1664 (3)	6630 (3)
C(24)	8677 (8)	-1703 (4)	7167 (3)
C(25)	8627 (8)	-1196 (4)	7564 (3)
C(26)	7810 (7)	-650 (3)	7432 (3)
C(30)	3089 (8)	2038 (3)	5931 (3)
C(31)	2232 (12)	2675 (4)	6041 (4)
C(32)	2011 (8)	1582 (4)	5630 (4)
C(33)	4361 (10)	2184 (3)	5520 (4)
O(4)	3508 (4)	-266 (2)	6088 (2)
N(40)	1270 (5)	-551 (3)	5786 (2)
C(41)	2682 (6)	-574 (3)	5754 (3)
C(42)	553 (7)	-146 (4)	6224 (3)
C(43)	343 (8)	-914 (4)	5380 (3)

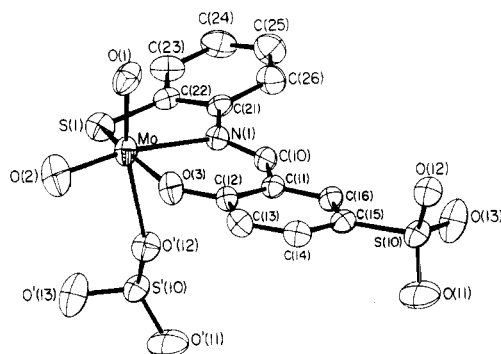
3,^{23,33–35} and **13**²³ have been previously reported. The remaining complexes are derivatives of these that have been ring-substituted in a manner so as to improve solubility and/or crystallinity. Complexes **1–12** are expected to contain six-coordinate Mo in solution; the designation solv = solvent allows for solvation and solvate substitution in different solvents. This investigation addresses the identity and reactivity of the products of the atom transfer reactions of $\text{Mo}^{\text{VI}}\text{O}_2$ complexes **1–6**. There having been no prior structural determination of these Mo(VI) Schiff base

(34) Topich, J. *Inorg. Chem.* **1981**, *20*, 3704.

(35) Dey, K.; Maiti, R. K.; Bhar, J. K. *Transition Met. Chem. (Weinheim, Ger.)* **1981**, *6*, 346.

Table V. Atom Positional Parameters ($\times 10^4$) for $\text{Mo}_2\text{O}_3(3\text{-OEtssp})_2(\text{DMF})_2\cdot 2\text{DMF}$

atom	<i>x/a</i>	<i>y/b</i>	<i>z/c</i>
O(2)	0	0	0
Mo(1)	507.7 (2)	1017.2 (1)	1407.2 (1)
O(1)	2321 (2)	840 (2)	1929 (2)
O(3)	1429 (2)	2431 (1)	761 (1)
N(1)	125 (2)	2196 (2)	2874 (2)
C(10)	276 (3)	3300 (2)	2937 (2)
C(11)	871 (3)	3967 (2)	2128 (2)
C(12)	1443 (3)	3520 (2)	1114 (2)
C(13)	2056 (3)	4307 (2)	420 (2)
C(14)	2035 (4)	5452 (2)	704 (3)
C(15)	1425 (5)	5875 (2)	1694 (3)
C(16)	866 (4)	5154 (2)	2392 (2)
O(11)	2628 (3)	3820 (2)	-522 (2)
C(17)	3170 (4)	4539 (3)	-1297 (3)
C(18)	3566 (6)	3777 (4)	-2301 (3)
S(1)	-1371.7 (8)	-338.1 (5)	2189.0 (5)
C(21)	-493 (3)	1694 (2)	3790 (2)
C(22)	-1280 (3)	510 (2)	3538 (2)
C(23)	-1962 (4)	-5 (3)	4390 (3)
C(24)	-1809 (5)	632 (3)	5468 (3)
C(25)	-949 (5)	1793 (3)	5722 (2)
C(26)	-294 (4)	2321 (2)	4882 (2)
O(4)	-1901 (2)	1562 (2)	814 (1)
C(41)	-2262 (3)	1482 (2)	-210 (2)
N(40)	-3740 (3)	1476 (2)	-670 (2)
C(43)	-4106 (4)	1245 (3)	-1884 (2)
C(42)	-5091 (4)	1573 (3)	7 (3)
C(51)	3243 (5)	5780 (4)	5160 (3)
N(50)	4262 (4)	6713 (3)	5789 (2)
C(53)	4199 (6)	6985 (4)	6977 (4)
C(52)	5400 (8)	7562 (6)	5344 (5)
O(50)	2210 (4)	5087 (3)	5472 (3)

**Figure 2.** Structure of $[\text{MoO}_2(5\text{-SO}_3\text{ssp})]^-$ as its Me_4N^+ salt (**4a**), showing 50% probability ellipsoids and the atom-labeling scheme.

complexes, two of them were crystallographically characterized.

Structures of Mo(VI) Complexes. Views of the structures of complexes **2** and **4a** are presented in Figures 1 and 2, respectively, and selected metric parameters are listed in Table VII. The structures are typical of dioxo-Mo(VI) complexes, in which the structural and electronic demands of the invariably *cis*- MoO_2 groups dominate the detailed stereochemistry. The bond distances (1.695 (2)–1.712 (2) Å) and angles (105°) of this group in the two complexes are within the usual ranges. Complex **2** crystallizes as a discrete molecule with a methanol ligand completing six-coordination. Complex **4a** is a chain polymer in which the six-coordination of Mo is completed by a sulfonato oxygen atom from an adjacent molecule.

The coordination geometry corresponds to a severely distorted octahedron. The anionic donor atoms are mutually trans and cis to the oxo ligands, and the weaker π -donors are trans to one of these ligands. Except for a few "skew-trapezoidal" molecules,³⁶ these structural features are invariant in dioxo-Mo(VI) complexes. The Schiff base ligands display *mer* coordination as found in

Table VI. Atom Positional Parameters ($\times 10^4$) for $\text{MoO}(3\text{-}i\text{-Bussp})(\text{bpy})\cdot\text{CD}_3\text{CN}$

atom	<i>x/a</i>	<i>y/b</i>	<i>z/c</i>
Mo(1)	3546.0 (3)	419 (1)	6205.5 (5)
O(1)	3785 (3)	-775 (12)	6769 (6)
S(1)	2937.1 (8)	-481 (5)	5957 (2)
O(3)	3877 (2)	2025 (12)	6210 (6)
N(1)	3302 (3)	1349 (11)	7195 (6)
N(5)	3815 (3)	-335 (16)	5149 (5)
N(4)	3329 (3)	1557 (12)	5012 (6)
C(10)	3420 (3)	2444 (13)	7576 (7)
C(41)	3494 (3)	1333 (14)	4302 (7)
C(42)	3400 (5)	2055 (19)	3589 (9)
C(43)	3126 (6)	2993 (22)	3576 (11)
C(44)	2972 (5)	3204 (20)	4299 (14)
C(45)	3076 (5)	2477 (17)	4994 (9)
C(51)	3762 (3)	298 (19)	4392 (7)
C(52)	3966 (4)	-91 (19)	3747 (7)
C(53)	4205 (4)	-1168 (23)	3883 (9)
C(54)	4253 (5)	-1762 (23)	4631 (14)
C(55)	4058 (4)	-1335 (19)	5243 (10)
C(11)	3723 (4)	3229 (14)	7397 (8)
C(12)	3952 (3)	2973 (14)	6754 (7)
C(13)	4265 (4)	3838 (16)	6676 (8)
C(14)	4324 (5)	4892 (17)	7229 (10)
C(15)	4085 (5)	5115 (19)	7851 (12)
C(16)	3803 (4)	4276 (15)	7945 (8)
C(30)	4513 (5)	3581 (19)	5987 (11)
C(31)	4842 (6)	4403 (27)	6048 (13)
C(32)	4291 (6)	3734 (25)	5150 (14)
C(33)	4665 (8)	2227 (31)	6047 (17)
C(21)	3000 (3)	696 (11)	7501 (6)
C(22)	2805 (3)	-195 (14)	6956 (7)
C(23)	2500 (4)	-850 (15)	7212 (9)
C(24)	2411 (4)	-673 (16)	8022 (10)
C(25)	2611 (4)	174 (15)	8568 (8)
C(26)	2902 (4)	839 (14)	8308 (8)
N(60)	1731 (6)	1470 (25)	443 (15)
C(61)	1680 (5)	1416 (19)	-281 (11)
C(62)	1616 (7)	1207 (27)	-1124 (15)

Table VII. Selected Distances (Å) and Angles (deg) for $\text{Mo}^{\text{VI}}\text{O}_2$ Complexes **2** and **4a**

	2	4a
Mo–O(1)	1.695 (2)	1.696 (3)
Mo–O(2)	1.712 (2)	1.700 (3)
Mo–O(3)	1.933 (2)	1.952 (3)
Mo–O(4)	1.961 (2)	
Mo–S(1)		2.407 (1)
Mo–N(1)	2.269 (2)	2.299 (3)
Mo–O'(12)		2.331 (3)
Mo–O(5)	2.353 (2)	
O(1)–Mo–O(2)	104.7 (1)	105.3 (2)
O(1)–Mo–O(3)	97.9 (1)	98.2 (2)
O(1)–Mo–N(1)	93.7 (1)	89.9 (2)
O(1)–Mo–O(4)	99.3 (1)	
O(1)–Mo–S(1)		96.3 (1)
O(2)–Mo–O(3)	102.8 (1)	103.2 (1)
O(3)–Mo–N(1)	80.6 (1)	83.4 (1)
O(4)–Mo–N(1)	74.8 (1)	
S(1)–Mo–N(1)		78.5 (1)
O(4)–Mo–O(2)	95.2 (1)	
S(1)–Mo–O(2)		90.3 (1)
O(1)–Mo–O(5)	171.7 (1)	
O(1)–Mo–O'(12)		164.4 (1)
O(3)–Mo–O(4)	151.0 (1)	
O(3)–Mo–S(1)		156.7 (1)
O(2)–Mo–N(1)	160.4	162.1 (2)

$[\text{MoOCl}_2(\text{sap})]^{1-}$.³⁷ In contrast, the *fac* arrangement is found in $\text{MoO}(\text{sap})(\text{cat})$.³⁸ Their oxygen and sulfur atoms are displaced back from the oxo atoms, as shown by the angles $\text{O}(3)\text{--Mo--O}(4)$

(36) Berg, J. M.; Spira, D. J.; Hodgson, K. O.; Bruce, A. E.; Miller, K. F.; Corbin, J. L.; Stiefel, E. I. *Inorg. Chem.* **1984**, *23*, 3412.

(37) Yamanouchi, K.; Yamada, S.; Enemark, J. H. *Inorg. Chim. Acta* **1984**, *85*, 129.
 (38) Mondal, J. U.; Schultz, F. A.; Brennan, T. D.; Scheidt, W. R. *Inorg. Chem.* **1988**, *27*, 3950.

Table VIII. Selected Torsional and Dihedral Angles (deg) for sap and ssp Ligands

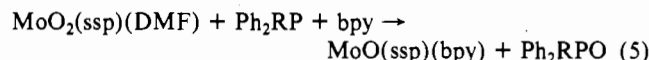
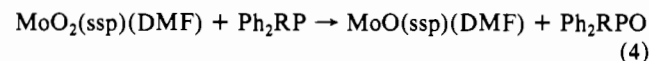
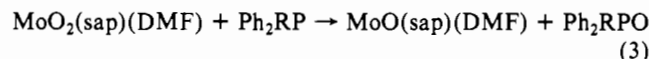
	2	4a	11	12	14
Torsional Angles ^a					
C(21)-N(1)-C(10)-C(11)	-176.1	172.9	179.6	179.6	177.7
N(1)-C(10)-C(11)-C(12)	-11.2	5.0	-3.0	-1.7	1.0
C(10)-N(1)-C(21)-C(22)	172.2	162.2	157.0	154.2	160.7
Dihedral Angle ^b					
C(11)-C(16)/C(21)-C(26)	19.8	17.4	24.4	29.1	20.0

^aThe torsional angle about bond B-C of atoms A-B-C-D is the angle that bond C-D is rotated from the A-B-C plane. The angle is positive if the rotation is clockwise when viewed along bond B-C (from B to C). ^bBetween benzene rings.

= 151.0 (1)° in **2** and O(3)-Mo-S(1) = 156.7 (1)° in **4a**. Metal-ligand distances cis to oxo atoms are unexceptional; Mo-O and Mo-S distances compare closely to those in related molecules.³⁷⁻³⁹ However, those bonds that are trans to the oxo ligands experience a lengthening owing to the well-recognized trans influence of multiply bonded oxometal groups. Thus the Mo-N(1) distances are least 0.1 Å longer than those in closely comparable Mo(V,IV) complexes where the trans influence is less or absent (vide infra). The Mo-O(5) (**2**; 2.353 (2) Å) and Mo-O'(12) (**4a**; 2.331 (3) Å) bonds are relatively long and the coordinated solvent molecules are labile, a behavior due in part to the trans effect.

The Schiff base ligands in **2** and **4a** and other complexes whose structures were determined in the work depart somewhat from planarity, as shown by the torsional and dihedral angles in Table VIII. Twists occur about three bonds, the largest about N(1)-C(21) in each case. The overall result of these conformations appears to be optimization of the three metal-ligand bond distances and relief of H(10)⋯H(26) interactions.

Oxo Transfer Reactions of Mo^{VI}O₂ Complexes. Boyd and Spence²³ reported reactions 3 and 4 (R = Et), from which Mo-containing products were isolated. When 2,2'-bipyridyl was present, reaction 5 resulted. The Mo(IV) product formulations



were supported by analytical data and electrochemical behavior. In addition, the nature of the product from reaction 3 was apparently sustained by its preparation in good yield under dinitrogen from Mo(IV) starting materials. Thereafter, Topich and Lyon^{12,13} determined the kinetics of reaction 4 in DMF solution. At 30 °C, $k \approx 10^{-3} \text{ M}^{-1} \text{ s}^{-1}$; the reaction is 11× faster at 60 °C. Neither complex reacts with less basic Ph₃P, and reaction 3 proceeds at a negligible rate at room temperature.

(a) Absorption Spectra. We have examined closely related reaction systems using the more soluble complexes **2** and **6** and Ph₂MeP⁴⁰ as the reductant, with the aims of establishing the reaction stoichiometry and isolating and crystallizing the Mo-containing product of each. Reactions analogous to 3 and 4 were monitored spectrophotometrically. As seen in Figures 3 and 4, an intense visible band develops near 450 nm and sharp isosbestic points are found. Both reactions proceeded to completion; that of **2** was considerably slower and under the stated conditions required 21 h at 70 °C. The reaction products of **2** and **6** have $\lambda_{\text{max}} = 307$ and 442 nm and $\lambda_{\text{max}} = 327$ and 453 nm, respectively. We have repeated reactions 3 and 4 (R = Me) on a preparative

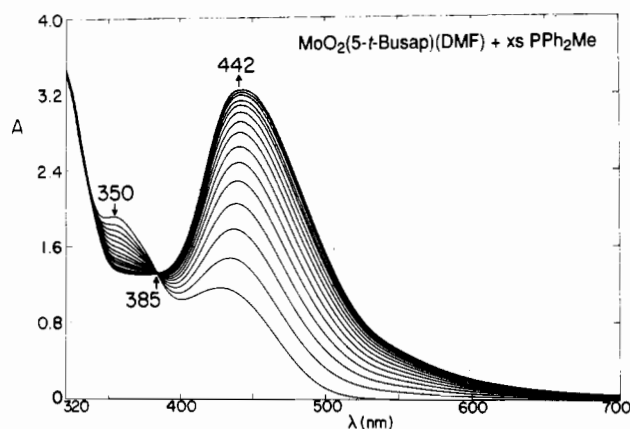


Figure 3. Reduction of MoO₂(5-*t*-Busap) (**2**; 22.7 mM) by a 20-fold excess of Ph₂MeP in DMF solution at 70 °C. Spectra were recorded every 90 min over 21 h. In this and the following figure, absorption maxima, isosbestic points, and the direction of absorbance changes (arrows) are indicated.

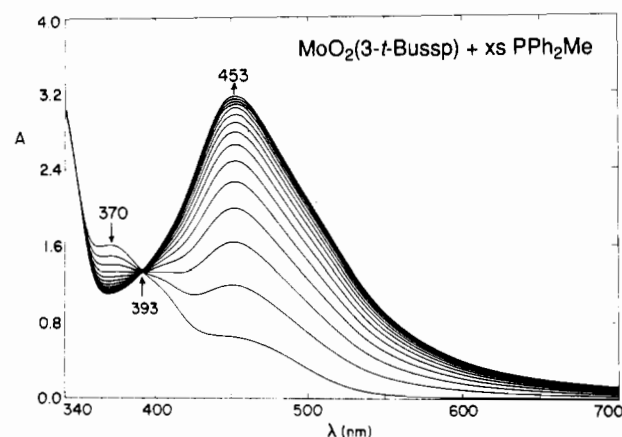


Figure 4. Reduction of MoO₂(3-*t*-Bussp) (**6**; 2.45 mM) by a 13-fold excess of Ph₂MeP in THF solution at 30 °C. Spectra were recorded every 45 min for 10.5 h.

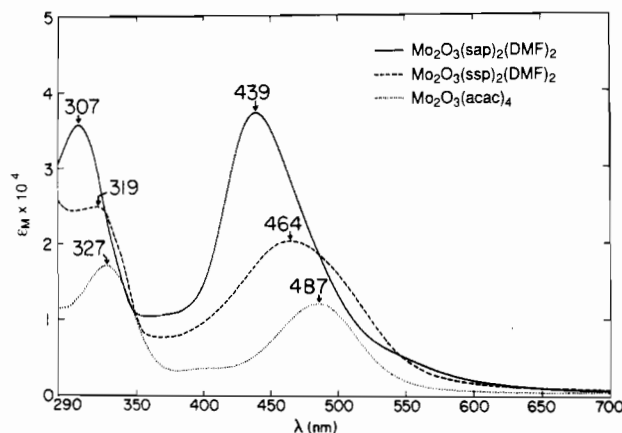


Figure 5. Absorption spectra of Mo₂O₃(acac)₄ in 1,2-C₂H₄Cl₂ solution and of Mo₂O₃(sap)₂(DMF)₂ (**7**) and Mo₂O₃(ssp)₂(DMF)₂ (**9**) in DMF solutions.

scale.²³ Absorption spectra of the isolated products are shown in Figure 5. Band maxima of isolated products are indistinguishable from those reported,²³ and the spectra are clearly similar to the final spectra of Figures 3 and 4. These observations support the proposition that reactions 3 and 4 and the reactions of Figures 3 and 4 yield analogous products.

(b) Stoichiometry. With a ³¹P NMR method introduced earlier,⁴¹ the stoichiometries of reactions analogous to 3-5 have

(39) (a) Berg, J. M.; Holm, R. H. *Inorg. Chem.* **1983**, *22*, 1768. (b) Berg, J. M.; Holm, R. H. *J. Am. Chem. Soc.* **1985**, *107*, 917 and references therein.

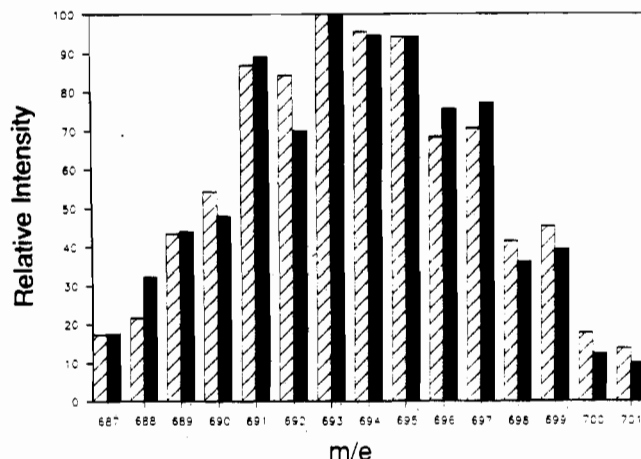
(40) Calorimetrically determined protonation enthalpies make it evident that the difference in intrinsic basicities of Ph₂EtP and Ph₂MeP is very slight: Bush, R. C.; Angelici, R. J. *Inorg. Chem.* **1988**, *27*, 681.

(41) Berg, J. M.; Holm, R. H. *J. Am. Chem. Soc.* **1984**, *106*, 3035.

Table IX. Stoichiometry of the Reactions of $\text{Mo}^{\text{VI}}\text{O}_2$ Complexes with Ph_2MeP

complex	solvent	<i>T</i> , K	$[\text{Ph}_2\text{MePO}]/[\text{Mo}^{\text{VI}}]_0^a$
1	DMF	340	0.51
3	DMF	300	0.46
4b	DMF	300	0.55
6	DMF	340	0.44
	THF	340	0.44
6 + bpy	THF	340	0.95
$\text{MoO}_2(\text{acac})_2$	1,2- $\text{C}_2\text{H}_4\text{Cl}_2$	340	0.53

^a $[\text{Ph}_2\text{MeP}]_0/[\text{Mo}^{\text{VI}}]_0 = 1.0\text{--}4.0$, $[\text{Mo}^{\text{VI}}]_0 = 10\text{--}60$ mM.

**Figure 6.** FAB mass spectrum of $\text{Mo}_2\text{O}_3(\text{ssp})_4$ (**9**, solv absent) in the parent ion region. The solid and shaded bars are calculated and observed relative intensities, respectively.

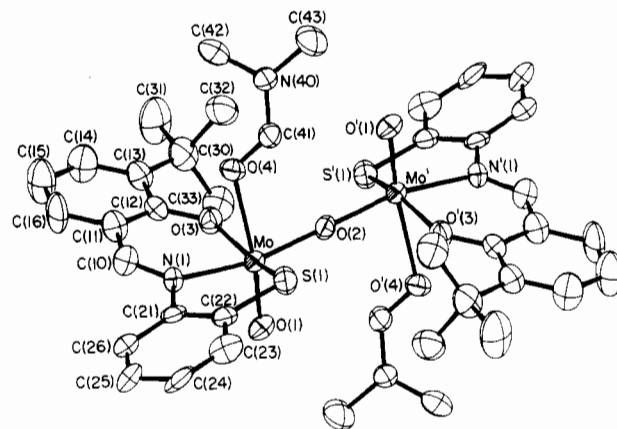
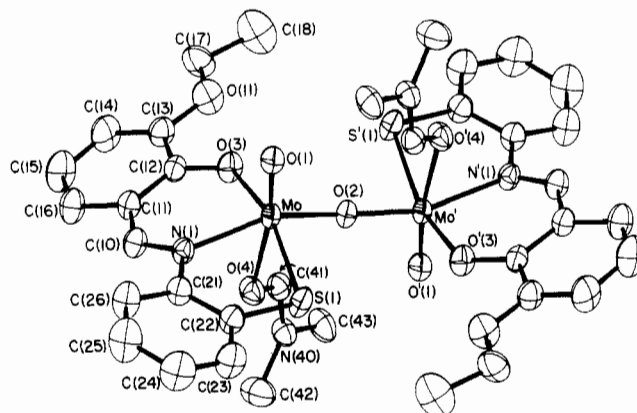
been investigated. In these experiments, the ratio of phosphine oxide to phosphine after completion of a reaction between a $\text{Mo}^{\text{VI}}\text{O}_2$ complex and Ph_2MeP , initially present in a known mole ratio, was determined from integrated signal intensities. The ratio *R* of phosphine oxide to initial Mo^{VI} concentration was calculated; results for four complexes and a control experiment with $\text{MoO}_2(\text{acac})_2$ are collected in Table IX. The data do not conform to generalized reaction 1 ($\text{X} = \text{Ph}_2\text{MeP}$), but are consistent with reaction 6, which is the sum of reactions 1 and 2 and requires *R*

$$2\text{MoO}_2\text{L}_n + \text{X} \rightarrow \text{Mo}_2\text{O}_3\text{L}_{2n} + \text{XO} \quad (6)$$

= 0.5. The control reaction affords *R* = 0.53; all other reaction systems except one are sufficiently close to 0.5 to establish this ratio. The exception is a system containing **6** and excess bpy, for which *R* = 0.95 is experimentally indistinguishable from the value of unity for reaction 5. The product of the control reaction is $\text{Mo}_2\text{O}_3(\text{acac})_4$, a known compound^{25,42} that has been further identified by mass spectrometry.⁴³ While its crystal structure has not been determined, that of closely related $\text{Mo}_2\text{O}_3(\text{acac})_2(\text{hfac})_2$ has been shown to possess an anti Mo_2O_3 group.⁴⁴

(c) Mass Spectrometry. The FAB mass spectrum of complex **9** in the $\text{M} + \text{H}^+$ region is shown in Figure 6. The peaks correspond to the solvate-free complex. Relative intensities are dominated by the Mo_2 isotope distribution. The agreement between calculated and observed relative intensities is adequate to establish the $\text{Mo}_2\text{O}_3(\text{ssp})_2$ formulation. Similar results have been obtained for complex **12**.

Structures of Phosphine Reduction Products. (a) Binuclear Mo(V) Complexes. In order to provide final identification of these products, the crystal structures of two of the six complexes obtained in this work by reduction of $\text{Mo}^{\text{VI}}\text{O}_2$ precursors with Ph_2MeP (in the absence of another ligand) have been determined. These have

**Figure 7.** Structure of $\text{Mo}_2\text{O}_3(3\text{-}t\text{-Bussp})(\text{DMF})_2$ (**11**), showing 50% probability ellipsoids and the atom-labeling scheme. Primed and unprimed atoms are related by an inversion center.**Figure 8.** Structure of $[\text{Mo}_2\text{O}_3(3\text{-EtOssp})_2(\text{DMF})_2] \cdot 2\text{DMF}$ (**12**), showing 50% probability ellipsoids and the atom-labeling scheme. Primed and unprimed atoms are related by an inversion center.**Table X.** Selected Distances (Å) and Angles (deg) for $\text{Mo}^{\text{V}}_2\text{O}_3$ Complexes **11** and **12**

	11	12
Mo–O(1)	1.683 (4)	1.678 (2)
Mo–O(2)	1.885 (0)	1.876 (0)
Mo–O(3)	2.034 (4)	2.030 (2)
Mo–S(1)	2.391 (2)	2.380 (1)
Mo–N(1)	2.164 (4)	2.162 (2)
Mo–O(4)	2.341 (4)	2.365 (2)
O(1)–Mo–O(2)	102.0 (1)	104.6 (1)
O(1)–Mo–O(3)	100.0 (2)	97.6 (1)
O(1)–Mo–S(1)	101.3 (2)	100.4 (1)
O(1)–Mo–N(1)	94.5 (2)	96.8 (1)
O(2)–Mo–O(3)	95.7 (1)	94.0 (1)
O(3)–Mo–N(1)	86.4 (2)	87.5 (1)
S(1)–Mo–O(2)	90.9 (1)	90.1 (1)
S(1)–Mo–O(3)	155.8 (1)	159.9 (1)
N(1)–Mo–O(2)	162.7 (1)	158.1 (1)
O(1)–Mo–O(4)	172.0 (2)	171.4 (1)

been shown to be $\text{Mo}_2\text{O}_3(3\text{-}t\text{-Bussp})_2(\text{DMF})_2$ (**11**) and $\text{Mo}_2\text{O}_3(3\text{-EtOssp})_2(\text{DMF})_2 \cdot 2\text{DMF}$ (**12**). Structures are shown in Figures 7 and 8, and selected bond distances and angles are collected in Table X.

Both complexes contain the $\text{Mo}^{\text{V}}_2\text{O}_3$ group with distorted octahedral coordination about the Mo atoms and have crystallographically imposed C_i symmetry, with the symmetry center located at the bridging oxo atom O(2). The same *mer* coordination of the tridentate ligands as in **2** and **4a** occurs, but with terminal atom O(2) replaced by bridge atom O(2). The O(1)–Mo–O(2) angles differ from those in the $\text{Mo}(\text{VI})$ complexes by less than 3°. For each complex, the Mo–O(2) distances are intermediate between the Mo–O(1) and Mo–O(3) distances, one consequence

(42) (a) Gehrke, H., Jr.; Veal, J. *Inorg. Chim. Acta* **1969**, *3*, 623. (b) Sobczak, J.; Ziolkowski, J. *J. Transition Met. Chem. (Weinheim, Ger.)* **1983**, *8*, 333.

(43) Chakravorty, M. C.; Bondyopadhyay, D.; Chaudhuri, M. K. *Int. J. Mass Spectrom. Ion Processes* **1986**, *68*, 1.

(44) Kamenar, B.; Korpar-Colig, B.; Penavic, M. *Cryst. Struct. Commun.* **1982**, *11*, 1583.

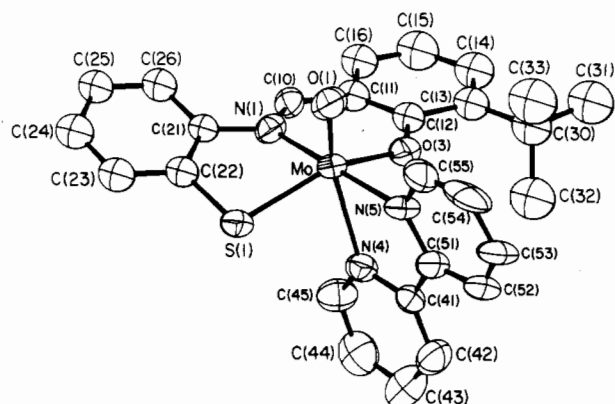


Figure 9. Structure of $[\text{MoO}(3\text{-}t\text{-Bussp})(\text{bpy})]\cdot\text{CD}_3\text{CN}$ (**14**), showing 50% probability ellipsoids and the atom-labeling scheme.

Table XI. Selected Distances (Å) and Angles (deg) for the $\text{Mo}^{\text{IV}}\text{O}$ Complex **14**

Mo–O(1)	1.695 (11)	Mo–N(1)	2.145 (10)
Mo–S(1)	2.384 (3)	Mo–N(4)	2.299 (11)
Mo–O(3)	2.038 (11)	Mo–N(5)	2.208 (9)
O(1)–Mo–S(1)	102.1 (4)	N(4)–Mo–O(3)	74.4 (4)
O(1)–Mo–O(3)	108.8 (5)	N(4)–Mo–N(1)	105.4 (4)
O(1)–Mo–N(1)	99.0 (4)	N(4)–Mo–N(5)	70.8 (4)
S(1)–Mo–O(3)	148.0 (3)	N(5)–Mo–O(1)	85.0 (5)
S(1)–Mo–N(1)	80.4 (3)	N(5)–Mo–S(1)	103.2 (3)
N(1)–Mo–O(3)	86.4 (4)	N(5)–Mo–O(3)	88.1 (5)
N(4)–Mo–O(1)	155.6 (4)	N(5)–Mo–N(1)	174.1 (5)
N(4)–Mo–S(1)	81.1 (3)		

of which is the absence of a clear trans influence of the bridge atom. As already noted, the Mo–N(1) distances are ca. 0.1 Å shorter than in **2** and **4a**. In these two complexes and in complex **14**, described below, the substantial torsional distortion about the N(1)–C(21) bond (Table VIII) is such as to displace atom S(1) away from the terminal oxo ligand. Other distances and angles are unexceptional.

(b) **Mononuclear Mo(IV) Complex.** Reduction of complex **6** in the presence of excess bpy afforded a green-black crystalline solid, ostensibly similar to the dark green product of reaction 5.²³ An X-ray structure determination showed the product to be the $\text{Mo}^{\text{IV}}\text{O}$ complex **14**, which crystallized as the acetonitrile monosolvate. The structure is presented in Figure 9; selected metric data are listed in Table XI. A strongly distorted octahedral stereochemistry and a *mer* disposition of the ssp ligand are again evident. The Mo–N(1) distance of 2.145 (10) Å is the shortest of any such distance in the five structures reported here, a property attributable to the absence of a trans anionic oxo ligand. The trans influence of atom O(1) is manifested in the Mo–N(4) bond length, which is 0.09 Å longer than that of Mo–N(5). Other structural aspects are unexceptional when compared with the preceding structures. The bpy bite angle of 70.8 (4)° is normal.

We have also repeated reaction 5 and obtained a dark green crystalline solid, whose absorption spectrum was not fully consistent with that reported for **13**.²³ However, as seen from the data in Table XII, the spectra of structurally authenticated **14** and our product of reaction 5 are very similar, thereby identifying the latter as **13**.

The foregoing results from reaction stoichiometries, mass spectrometry, and crystallography establish the products of reduction of $\text{Mo}^{\text{VI}}\text{O}_2$ species by oxo transfer as $\text{Mo}^{\text{V}}\text{O}_3$ complexes, which are formed under the stoichiometry of reaction 6 ($L = \text{sap}$, ssp, and their derivatives). It seems unlikely that any solvated $\text{Mo}^{\text{IV}}\text{O}$ sap or ssp complex has ever been isolated. We conclude that the product of reaction 5 is correctly formulated; i.e., the MoO(ssp) unit, and the MoO(sap) unit as well,²³ can be trapped by excess bpy upon their formation by oxo transfer. Presumably, MoOL(phen) ($L = \text{sap}$, ssp)²³ were formed in a similar fashion. We have established that the only observable chromophore produced over the course of reaction in the system initially containing

Table XII. ^1H NMR and Absorption Spectral Data for $\text{Mo}^{\text{VI}}\text{O}_2$, $\text{Mo}^{\text{V}}\text{O}_3$, and $\text{Mo}^{\text{IV}}\text{O}$ Complexes

complex	$\delta(\text{HC}=\text{N})$, ppm	λ_{max} , nm (ϵ_{M} , $\text{M}^{-1}\text{cm}^{-1}$)
$\text{Mo}^{\text{VI}}\text{O}_2$ 1 ^a	9.40	349 (9430), 421 (5670)
2	9.32 ^b	350 (9800), 422 (5580) ^c
3	9.09 ^d	374 (6070), 452 (sh, 1360) ^a
4b	9.13 ^b	375 (5920), 455 (sh, 1530) ^a
5 ^a	9.03	410 (sh, 3400), 481 (sh, 1000)
$\text{Mo}^{\text{V}}\text{O}_3$ 6 ^d	9.15	370 (6600), 453 (sh, 2210)
7 ^a	9.43, 9.44 ^e	307 (37200), 439 (38700)
8	8.70 ^{h,j}	307 (35000), 442 (35000) ^{a,h}
9	9.18, 9.22 ^{e,g,h}	319 (24700), 464 (20200)
10 ^a	9.31, 9.39 ^{d,g}	
11 ^d	9.32, 9.34 ^{e,h}	317 (35500), 464 (29400)
12 ^a	9.29, 9.32 ^{c,g,h}	
$\text{Mo}_2\text{O}_3(\text{acac})_2$ ^f	9.27 ^{g,h}	327 (30900), 453 (24300)
$\text{Mo}^{\text{IV}}\text{O}$ 13 ^a	9.29, 9.33 ^e	337 (34100), 464 (19100)
14 ^d	<i>i</i>	327 (17400), 487 (12100)
		308 (27300), 420 (8900), 466 (7750), 610 (sh, 4300), 683 (6220)
	9.30	306 (27400), 431 (10300), 476 (9300), 706 (8200)

^a DMF. ^b Me_2SO . ^c MeOH. ^d THF. ^e Pyridine. ^f 1,2- $\text{C}_2\text{H}_4\text{Cl}_2$; additional bands at 410 (3700) and 748 (600) nm. ^g Isolated solid. ^h Generated in situ. ⁱ Not measured. ^j Broad, may be a phosphine adduct; MeCN.

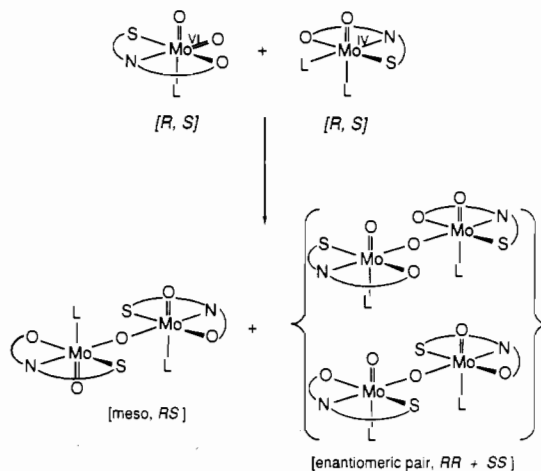


Figure 10. Schematic formation of $\mu\text{-oxo-Mo(V)-ssp}$ complexes from chiral (*R, S*) Mo(VI,IV) precursors.

3 mM **6** with 15 equiv of bpy and 25 equiv of Ph_2MeP in THF at 40 °C is the Mo(IV) product **14**. Because under these conditions the reaction of $\mu\text{-oxo}$ dimer **11** with bpy is much slower than this, **14** did not arise in major part by the cleavage of **11** by bpy. Owing to our inability to generate concentrations of solvated Mo(IV) complexes separately or in an equilibrium, we have been unable to measure their rates of reaction with MoO_2 species and with bpy.

Stereochemistry of Formation of $\mu\text{-Oxo-Mo(V)}$ Dimers. The formation of such species is schematically illustrated with ssp complexes in Figure 10 and is discussed with reference to generalized reactions 1 and 2. The bpy trapping experiments support a solvated $\text{Mo}^{\text{IV}}\text{O}$ complex, whose structure is assumed to follow that of **14**, as the *instantaneous* product of oxo transfer (reaction 1). In the next step (reaction 2), $\text{Mo}^{\text{VI}}\text{O}_2$ and $\text{Mo}^{\text{IV}}\text{O}$ complexes undergo inner-sphere electron transfer with retention of the $\mu\text{-oxo}$ bridge, yielding $\text{Mo}^{\text{V}}\text{O}_3$ products. The structures of Mo(VI,IV)-ssp complexes⁴⁵ emphasize the ease of reaction 2. The ssp

(45) Other than the molybdenum dithiocarbamates,^{17,46} complexes of ssp are the only ones in which structures of the $\text{Mo}^{\text{VI}}\text{O}_2$, $\text{Mo}^{\text{V}}\text{O}_3$, and $\text{Mo}^{\text{IV}}\text{O}$ forms have been determined.

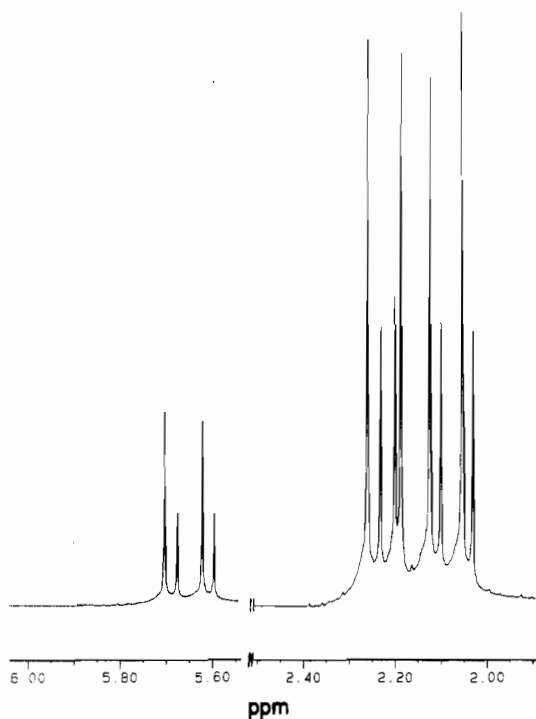


Figure 11. ^1H NMR spectrum of $\text{Mo}_2\text{O}_3(\text{acac})_4$ in CDCl_3 solution, showing the existence of diastereomers.

ligand has the same *mer* arrangement in reactants and products, with the result that dimer formation requires only displacement of solvent at Mo(IV) and lengthening one and making another Mo–O bond concomitant with electron transfer. Adjustments of O–Mo–O angles and other dimensions are relatively minor. In the current systems, reaction 2 is rapid and irreversible.

Because the Mo(VI,IV) reactants are chiral, the product complexes of reaction 2 can be formed as meso and racemic diastereomers.⁴⁷ Products **11** and **12** are among those structurally established Mo(V) complexes with imposed or idealized C_i symmetry and an anti conformation of the Mo_2O_3 group.^{17,18,20,21,44} While certain of these complexes with both unidentate and chelate ligands are achiral,²¹ others,^{17,18,20,44} including **11** and **12**, contain chiral “half-dimers”. All complexes with idealized or imposed C_2 symmetry^{17–19} have the syn conformation and also contain chiral half-dimers. In one case, both C_i and C_2 forms of the same compound occur in the same crystal,¹⁷ and in another case the two forms could be prepared separately.¹⁸ These isomers are not interconvertible by rotation about a bridge Mo–O bond.

Detection of diastereomeric Mo_2O_3 complexes was first shown with $\text{Mo}_2\text{O}_3(\text{acac})_4$, which was prepared as described by Chen et al.²⁵ Each chiral half-dimer contains two inequivalent ring protons and four inequivalent methyl groups. The spectrum of the complex in chloroform, shown in Figure 11, exhibits sets of doubled ring proton (near 5.7 ppm) and methyl group resonances (centered at 2.15 ppm) in an intensity ratio within each set of ca. 2:1. Evidently, the two diastereomers are not formed in equal amounts and/or are partially separated in the workup procedure.

The time course of the reaction between complex **4b** and Ph_2MeP in methanol solution is displayed in Figure 12, in which azomethine proton signals are monitored. The singlet of the Mo(VI) complex at 9.10 ppm diminishes with time and is ultimately replaced by two essentially equally intense resonances at 9.27 and 9.30 ppm. The final spectrum is the same as that of the isolated solid. In four of the six cases listed in Table XII, doubled signals of nearly equal intensity are observed with separations of 0.02–0.08 ppm for complexes generated in situ by

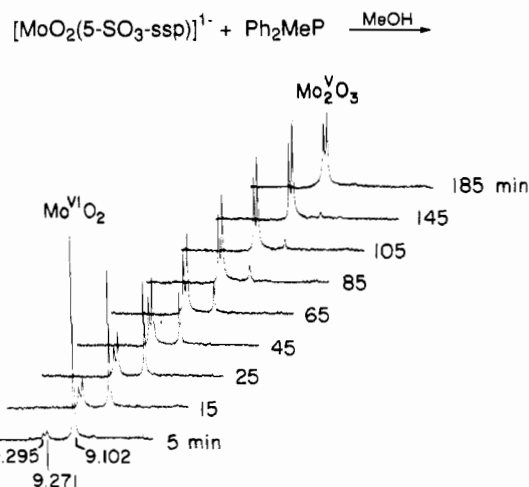


Figure 12. ^1H NMR spectra of a reaction mixture consisting initially of 21 mM $[\text{MoO}_2(5\text{-SO}_3\text{ssp})]^{1-}$ (**4b**) and 1.5 equiv of Ph_2MeP in methanol- d_4 solution in the azomethine region. Chemical shifts of the Mo(VI) reactant and the Mo(V) product are indicated.

reduction with Ph_2MeP (to avoid fractionation of isomers) or isolated from the reaction mixture and redissolved. These results are interpreted in terms of formation of both diastereomers in reaction 2. In the two instances (**8**, **11**) where signal splitting is not found with complexes generated in situ, it is probable that chemical shift differences are beyond resolution, even at 500 MHz. Recall that the μ -oxo structure of **11** has been established by X-ray diffraction. It was the observation of doubled azomethine proton signals upon reduction of Mo(VI) complexes with phosphines that provided the initial indication that the products were not mononuclear Mo(IV) species.

Criteria for Detection of the Mo_2O_3 Bridge Unit. Because of the pervasiveness of this unit in Mo oxo transfer chemistry, simple means of its detection short of an X-ray structural determination are desirable. Mass spectrometry is an obvious technique to apply to suitably stable compounds. A distinction can be made between forward or reverse reactions 1 and 6 from determination of reaction stoichiometries, but the method will fail unless forward reaction 2 is fast and irreversible. Detection of diastereomeric reaction products is suggestive of the formation of the Mo_2O_3 unit, but bridged binuclear $\text{Mo}^{\text{IV}}\text{O}$ complexes with syn and anti oxo arrangements are conceivable (but not yet known).

Schiff base complexes containing the Mo_2O_3 group with combinations of N and anionic O and S ligands tend to reveal rather distinctive absorption spectra, as shown by the data in Table XII and the examples in Figure 5. In these instances, an intense visible band appears at 440–490 nm and a band or shoulder appears at 300–340 nm. The diagnostic value of these spectra was shown by using compound **9**. The same crystal used in the X-ray structure determination gave a solution absorption spectrum with the band maxima in Table XII. Lincoln and Koch,¹⁸ in their study of the isomers of $\text{Mo}_2\text{O}_3\text{Cl}_2(\text{HB}(\text{pz})_3)_2$, noted that an earlier criterion of a purple color and a visible band near 500 nm as diagnostic of Mo_2O_3 complexes is unduly restrictive. At the time of its proposal,⁴⁸ the great majority of spectral data were available for dithiocarbamate⁴⁹ and related sulfur chelate complexes,⁵⁰ whose behavior is somewhat complicated by equilibrium 2. More recent data on dithiocarbamates⁵¹ and on thiolate complexes,^{14,52} which are also purple, indicate correlation of the Mo_2O_3 structure with spectra displaying principal bands at 330–380 and 500–515 nm.

(48) Stiefel, E. I. *Prog. Inorg. Chem.* **1977**, *22*, 1.

(49) Newton, W. E.; Corbin, J. L.; Bravard, D. C.; McDonald, J. W. *Inorg. Chem.* **1974**, *13*, 1100.

(50) (a) Newton, W. E.; Corbin, J. L.; McDonald, J. W. *J. Chem. Soc., Dalton Trans.* **1974**, 1044. (b) Chen, G. J. J.; McDonald, J. W.; Newton, W. E. *Inorg. Nucl. Chem. Lett.* **1976**, *12*, 697.

(51) Pandeya, K. B.; Kaul, B. B. *Syn. React. Inorg. Met.-Org. Chem.* **1982**, *12*, 259.

(52) Pickett, C.; Kumar, S.; Vella, P. A.; Zubieta, J. *Inorg. Chem.* **1982**, *21*, 908.

(46) (a) Ricard, L.; Estienne, J.; Karagiannidis, P.; Toledano, P.; Fischer, J.; Mitschler, A.; Weiss, R. *J. Coord. Chem.* **1974**, *3*, 277. (b) Berg, J. M.; Hodgson, K. O. *Inorg. Chem.* **1980**, *19*, 2180.

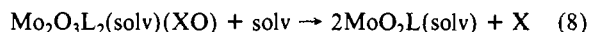
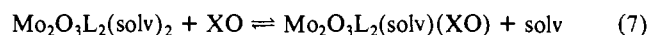
(47) In accounting for isomers, we assume chiral ligand conformations to be rapidly racemized.

$\text{Mo}_2\text{O}_3\text{Cl}_2(\text{HB}(\text{pz})_3)_2$ is yellow-brown with a strong band at 460 nm, in the range of the present set of compounds. $\text{Mo}_2\text{O}_3(\text{acac})_4$ and the Mo(V) Schiff base complexes examined here form dark red-orange and red-brown solutions, respectively. The latter show a characteristic two-band pattern that is strongly blue-shifted compared to spectra of complexes with anionic sulfur ligands. Perhaps the simplest chromophore of this type is $\text{Mo}_2\text{O}_3\text{Cl}_4(\text{DMF})_4$, formulated by analogy with structurally proven $\text{Mo}_2\text{O}_3\text{Cl}_4(\text{py})_4$.^{21c} It was generated in situ in DMF solution by the reaction of MoO_2Cl_2 with $1/2$ equiv of Ph_2MeP and shows a prominent band at 461 nm and a shoulder at 306 nm.

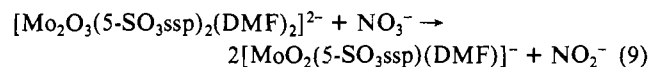
From a combination of the preceding chemical and spectroscopic methods, it should prove possible to detect the formation of Mo_2O_3 complexes. Other possible methods, such as ^{17}O and ^{95}Mo NMR^{53,54} and resonance Raman spectroscopy, have not been investigated adequately enough to know if intrinsic chemical shifts or vibrational frequencies are sufficiently independent of ligands to render them structurally diagnostic.

Reactions of Mo_2O_3 Complexes. (a) Stoichiometry. In order to assess the oxo transfer behavior of such complexes, a series of reactions in DMF solutions was carried out with **7**, **10**, and **11**. In the first set of reactions, which were monitored spectrophotometrically, complexes **7** and **11** were treated with excess Ph_2SO in DMF solution. These were cleanly and completely converted to **1** and **6**, respectively. Spectral changes were the reverse of the reduction reactions in Figures 3 and 4; the same tight isosbestic points were observed. Product stoichiometry was established by ^{19}F NMR experiments. A 7 mM solution of **7** was reacted with 2 equiv of $(\text{R}_F)_2\text{SO}$ ($\text{R}_F = p\text{-C}_6\text{H}_4\text{F}$) at 100 °C for 10 min. The $[\text{Mo}_2\text{O}_3\text{L}_2(\text{DMF})_2]_0:(\text{R}_F)_2\text{S}$ mole ratio, determined by integration of the sulfoxide (-109 ppm) and sulfide (-115 ppm) signals, was 0.99. For a system initially containing 13 mM **10** and **6** equiv of sulfoxide and allowed to react for 4 days at room temperature, the ratio was 1.03. Both experiments were performed in duplicate.

The collective results demonstrate that sulfoxides, and presumably other substrates, are reduced with a stoichiometry corresponding to the reverse reaction 6. Any $\text{Mo}^{\text{IV}}\text{O}$ complex present in equilibrium 2 would also reduce sulfoxide. However, we have never been able to detect any NMR signals due to $\text{Mo}^{\text{IV}}\text{O}_2$ species in any solution prepared from **7-12** by using a variety of solvents including DMF, MeOH, THF, and pyridine. It appears likely that the substrate reacts directly with the binuclear complexes by displacement of labile solvent followed by atom transfer, as in generalized reactions 7 and 8.



(b) Reduction of Nitrate. As a further example of the apparent reactivity of Mo_2O_3 complexes, the reaction of **10** and excess nitrate in DMF solution in the presence of sulfamic acid was examined. The reaction was monitored spectrophotometrically as shown in Figure 13. The intense band of **10** at 464 nm decreases with time, a clean isosbestic point at 396 nm is evident, and the final spectrum is identical with that of **4b** (Table XII). Dinitrogen, arising from the scavenging reaction $\text{H}_2\text{NSO}_3\text{H} + \text{NO}_2^- \rightarrow \text{N}_2 + \text{HSO}_4^- + \text{H}_2\text{O}$, required to suppress reaction of nitrite with the Mo complexes, was detected¹¹ in the head space of the reaction vessel. The process observed is the nitrate reduction reaction 9, and is one of the few abiological reductions of nitrate



mediated at a Mo center. This overall reaction presumably proceeds by the sequence of reactions 7 and 8. Complex **11** was also shown to reduce nitrate in a reaction analogous to (9). Mononuclear Mo(V) complexes reduce nitrate to nitrogen dioxide rather than nitrite by the minimal reaction³ $[\text{Mo}^{\text{V}}\text{O}]^{3+} + \text{NO}_3^-$

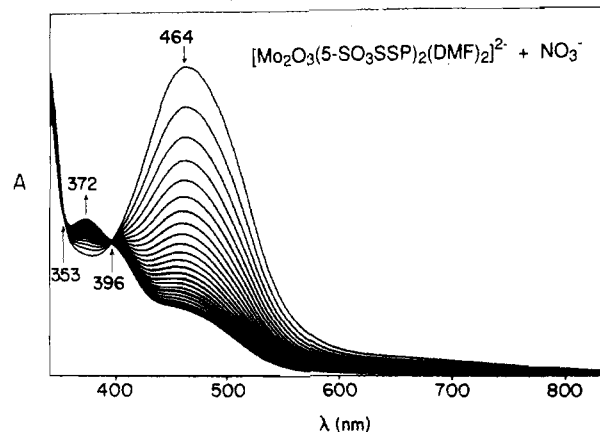


Figure 13. Reduction of nitrate to nitrite at 25 °C in a DMF solution containing $[\text{Mo}_2\text{O}_3(5\text{-SO}_3\text{ssp})_2]^{2-}$ (**10**). Spectra were recorded every 4 min over 116 min. Initial concentrations: $[\text{10}] = 0.27$ mM; $[\text{NO}_3^-] = 2.1$ mM; $[\text{H}_2\text{NSO}_3\text{H}] = 0.98$ mM.

$\rightarrow [\text{MoO}_2]^{2+} + \text{NO}_2$, which requires intermolecular electron and atom transfer. In reaction 9, atom transfer is intermolecular and electron transfer intramolecular. Oxo transfer reduction of nitrate to nitrite by a binuclear Mo(III) complex has been demonstrated.⁵⁵ We have recently reported the stoichiometric reduction of nitrate to nitrite by the reverse of reaction 1,¹¹ which under our oxo transfer hypothesis for the mechanism of action of certain molybdoenzymes⁹ provides a plausible reaction pathway for nitrate reductases.

Summary. This investigation has demonstrated that reduction of the $\text{Mo}^{\text{VI}}\text{O}_2$ Schiff base complexes **1-6** by oxo transfer yields the binuclear diastereomeric $\text{Mo}^{\text{V}}\text{O}_2$ complexes **7-12**. To account for the sharp isosbestic points in this (Figures 3 and 4) and other work,^{12,13} μ -oxo dimer formation reaction 2 must be fast and complete, factors that appear to be favored by the structures of $\text{Mo}^{\text{VI}}\text{O}_2$ and $\text{Mo}^{\text{IV}}\text{O}$ complexes. It is unlikely that any mononuclear Mo(IV) complex of the type $\text{MoOL}(\text{solv})$ ($\text{L} = \text{sap}, \text{ssp}$) has ever been isolated. However, the MoOL entity can be trapped with bpy, as in **13** and **14**, justifying the Mo(IV) formulations given elsewhere for the instantaneous products of oxo transfer from MoO_2 complexes.^{3,7,9} Previously determined second-order rate constants for reactions such as (4)^{12b,13} are unaffected by product formulation. Criteria are offered for the detection of the Mo_2O_3 unit. Evidence has been presented that complexes containing this unit, in solutions where dimer dissociation is not detectable (by ^1H NMR), function as intact oxo transfer reductants toward substrates such as sulfoxides and nitrate. Lastly, the results of this investigation emphasize the pervasiveness of dimerization reaction 2. There are no oxo transfer systems in which this reaction does not occur, either irreversibly or as an equilibrium, unless suppressed by steric factors or added ligands.⁵⁶ Properties of equilibrium dimerization reactions are summarized elsewhere.³ Sterically bulky complexes designed to eliminate dimerization have been prepared.^{15,39b,57,58}

Acknowledgment. This research was supported by NSF Grant CHE 85-21365. X-ray diffraction equipment was obtained through NIH Grant 1 S10 RR-02247. We thank P. Briggs for mass spectrometry determinations.

Supplementary Material Available: Listings of crystallographic data including details of data collection, positional and thermal parameters, interatomic bond distances and angles, and calculated hydrogen atom positions for compounds **2**, **4a**, **11**, **12**, and **14** (28 pages); tables of calculated and observed structure factors for **2**, **4a**, **11**, **12**, and **14** (88 pages). Ordering information is given on any current masthead page.

(53) Miller, K. F.; Wentworth, R. A. D. *Inorg. Chem.* **1980**, *19*, 1818.
(54) Minelli, M.; Enemark, J. H.; Brownlee, R. T. C.; O'Connor, M. J.; Wedd, A. G. *Coord. Chem. Rev.* **1985**, *68*, 169.

(55) Wiegardt, K.; Woeste, M.; Roy, P. S.; Chaudhuri, P. *J. Am. Chem. Soc.* **1985**, *107*, 8276.
(56) Kaul, B. B.; Enemark, J. H.; Merbs, S. L.; Spence, J. T. *J. Am. Chem. Soc.* **1985**, *107*, 2885.
(57) Subramanian, P.; Spence, J. T.; Ortega, R.; Enemark, J. H. *Inorg. Chem.* **1984**, *23*, 2564.
(58) Cook, C. J.; Topich, J. *Inorg. Chim. Acta* **1988**, *144*, 81.